

On the Performance of IRS-Aided NOMA in Interference-Limited Networks

Salah Almaghthawi^{ID}, *Graduate Student Member, IEEE*, Emad Alsusa^{ID}, *Senior Member, IEEE*, and Arafat Al-Dweik^{ID}, *Senior Member, IEEE*

Abstract—This letter investigates the performance of intelligent reflecting surface (IRS) aided downlink power-domain non-orthogonal multiple access (NOMA) in Nakagami- m fading channels with cochannel interference (CCI). Using the Gamma approximation, we derive closed-form expressions for the ergodic capacity and outage probability, while taking CCI into account. The analytical results, validated through Monte Carlo simulation, show that IRS-aided NOMA is superior to the IRS-OMA counterpart, and that the Gamma distribution closely approximates the cascaded Nakagami- m distribution. The results are presented for various number of users and reflecting elements.

Index Terms—Intelligent reflecting surface, non-orthogonal multiple access, Ergodic capacity, outage probability, Nakagami- m fading, Gamma approximation, co-channel interference.

I. INTRODUCTION

INTELLIGENT reflecting surfaces (IRSs) have been identified as a potential solution to manipulate the radio propagation environment in mobile communication networks beyond the fifth generation (B5G) [1], [2]. Generally, an IRS panel consists of an array of reflecting elements that can dynamically alter the phases and amplitudes of the incoming signals to coherently combine and forward them to the receiver [3], [4]. An IRS panel can be mounted on a tall building or an unmanned aerial vehicle (UAV) and hence can provide a means to create a virtual line-of-sight (LOS) link between a basestation (BS) and the users, enabling smart radio environments where blockages can be readily overcome. Likewise, Non-orthogonal multiple access (NOMA) has been widely considered as a key enabler to meet the extraordinary quality of service (QoS) requirements of future mobile communication networks. This is because NOMA can provide several important features, such as improving spectrum efficiency, supporting massive user connections, and facilitating fairness among users [5], [6].

Manuscript received 20 October 2023; accepted 20 November 2023. Date of publication 27 November 2023; date of current version 9 February 2024. The associate editor coordinating the review of this article and approving it for publication was Y. Fu. (*Corresponding author: Salah Almaghthawi*.)

Salah Almaghthawi is with the Department of Electrical and Electronic Engineering, The University of Manchester, M13 9PL Manchester, U.K., and also with the Department of Electrical Engineering, Islamic University of Madinah, Madinah 41411, Saudi Arabia (e-mail: salah.almaghthawi@postgrad.manchester.ac.uk).

Emad Alsusa is with the Department of Electrical and Electronic Engineering, The University of Manchester, M13 9PL Manchester, U.K. (e-mail: e.alsusa@manchester.ac.uk).

Arafat Al-Dweik is with the 6G Research Center, Khalifa University, Abu Dhabi, UAE (e-mail: dweik@fulbrightmail.org).

Digital Object Identifier 10.1109/LWC.2023.3336800

Several articles have recently investigated the integration of IRS and NOMA. For example, the authors in [7] have examined the performance of IRS-assisted NOMA and IRS-OMA networks in terms of ergodic capacity and outage probability. In [8], moment matching is adopted to derive the distribution of the end-to-end channel gains, and showed that they follow the Gamma distribution, to evaluate the average block error rate (BLER) of IRS-NOMA for short packet communications. The authors in [9] analyzed the outage probability and ergodic capacity of IRS-assisted UAV networks using NOMA. In addition, the authors in [10] studied the impact of coherent phase shift and random discrete shift on the outage probability of an IRS-NOMA network, while in [11], the authors investigated the outage probability of an IRS-assisted cognitive radio network. Furthermore, a novel IRS design is proposed in [12] to improve the physical layer security aspect of IRS-aided NOMA. In [13], the outage probability and ergodic capacity of IRS-NOMA is studied where perfect and imperfect successive interference cancelation (SIC) are considered. Unlike [13], which evaluates the performance under residual interference, this letter focuses on the impact of cochannel interference (CCI). Furthermore, unlike [8] where only Rayleigh fading is assumed, this letter considers a Nakagami- m fading, which includes Rayleigh fading as a special case.

Motivated by the potential benefits of IRS and NOMA, we investigate the impact of integrating these two technologies in scenarios where blockages between BS and users exist, and evaluate the performance by deriving closed-form expressions for the ergodic capacity and outage probability for Nakagami fading channels with CCI. In particular, we adopt the Gamma approximation to represent the cascaded Nakagami- m distribution with the assumption that all users suffer from independent and identically distributed (i.i.d) CCI. The accuracy of the derived expressions is confirmed by matching Monte Carlo simulation.

The remainder of this letter is structured as follows. Section II presents the proposed IRS-NOMA system configuration. Section III presents the derived analytical closed-form expressions for the ergodic capacity and outage probability. Section IV presents the numerical results and validates the derived expressions using Monte Carlo simulation, and finally Section V concludes this letter.

II. SYSTEM MODEL

The considered IRS-aided downlink NOMA communication network is shown in Fig. 1, where a BS communicates simultaneously with K users, U_1, U_2, \dots, U_K via an IRS that has N elements. The BS and user terminals are considered

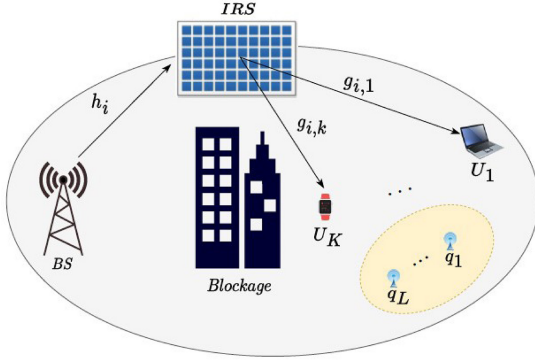


Fig. 1. IRS-aided downlink NOMA system.

to be equipped with a single antenna. Using NOMA, the BS transmits the superposition-coded signal $s = \sum_{k=1}^K \sqrt{\beta_k P} s_k$ to all users, where P indicates the total transmission power, which is normalized to unity, s_k is the information-bearing signal of U_k and β_k is the power allocation coefficient, $\sum_{k=1}^K \beta_k = 1$. In IRS-based networks, it is typically assumed that the direct link between the BS and users is severely attenuated. In addition, we consider a heterogeneous network where all users are affected by i.i.d CCI from a neighboring indoor femtocell [14]. The fading channel between the BS and the i th reflecting element is denoted as $h_i = d_s^{-\frac{\lambda}{2}} \tilde{h}_i$, $i = \{1, 2, \dots, N\}$, where \tilde{h}_i denotes the small scale fading and d_s is the distance between BS and IRS. Similarly, the channel between the IRS and the user terminal is represented as $g_{i,k} = d_{U_k}^{-\frac{\lambda}{2}} \tilde{g}_{i,k}$ where $\tilde{g}_{i,k}$ denotes the small-scale fading and d_{U_k} is the distance between the IRS and the k th user.

Without loss of generality, all channels are assumed to undergo Nakagami- m and large-scale fading with path loss exponent λ . Under the assumption of perfect knowledge of the channel phases, θ_{h_i} and $\theta_{g_{i,k}}$, the adjustable phase shift induced by the i th reflecting element is chosen such that $\theta_i = -(\theta_{h_i} + \theta_{g_{i,1}})$. This leads to achieving the maximum instantaneous SNR for the cell-edge user, i.e., U_1 . The channel coefficient for the interference link between users and the l th interfering signal is denoted as $q_{l,k} = d_{L_l}^{-\frac{\lambda}{2}} \tilde{q}_{l,k}$, where d_{L_l} is the distance between l th interferer and end-users, and $\tilde{q}_{l,k}$ denotes the small scale fading and is assumed to follow Nakagami- m fading as it closely represents many distributions by varying the shape parameter m in the range of $0.5 \leq m \leq \infty$.

Therefore, the received signal reflected by the IRS at the k th user is given by

$$y_k = \underbrace{\sum_{i=1}^N h_i g_{i,k} \alpha_i e^{j\theta_i} s}_{\text{Desired signal}} + \underbrace{\sqrt{P_I} \sum_{l=1}^L q_{l,k} x_l}_{\text{CCI Signal}} + w_k \quad (1)$$

where x_l and P_I represent the information symbol and power of the CCI, respectively. Furthermore, α_k represents the attenuation factor of the reflecting element, which is normalized to unity. The variable w_k denotes the additive white Gaussian noise (AWGN), $w_k \sim \mathcal{CN}(0, \sigma_w^2)$.

For NOMA with perfect SIC, assuming that the noise remains Gaussian after SIC [15], the signal-to-interference-plus-noise ratio (SINR) at the k th user to decode the j th user information, ($k \geq j$) is written as

$$\vartheta_{k \rightarrow j} = \frac{\rho \beta_j \chi_{1,k}}{\rho \chi_{1,k} \sum_{i=j+1}^K \beta_i + \rho \chi_{2,k} + 1} \quad (2)$$

where $\rho = \frac{P}{\sigma^2}$ is the transmit signal power to noise ratio (SNR), $\rho_I = \frac{P_I}{\sigma^2}$, and the noise power is assumed to be normalized to unity, $\chi_{1,k} \triangleq (\sum_{i=1}^N |h_i| |g_{i,k}|)^2$, and $\chi_{2,k} \triangleq \sum_{l=1}^L |q_{l,k}|^2$. Furthermore, the effective cascaded channel gains are ordered as $\chi_{1,1} \leq \chi_{1,2} \leq \dots \leq \chi_{1,K}$ and $d_{U_1} > d_{U_2} > d_{U_K}$. After invoking SIC and canceling $K-1$ user's signals, the received SINR at the k th user is written as

$$\vartheta_K = \frac{\rho \beta_K \chi_{1,K}}{\rho \chi_{2,K} + 1}. \quad (3)$$

III. PERFORMANCE ANALYSIS

A. Ergodic Capacity

In this section we derive the closed-form expression for the ergodic capacity of the considered IRS-NOMA system. Although the closed-form expression of the probability distribution function (PDF) for the cascaded Nakagami- m $|h_i| |g_{i,k}|$ can be obtained, it is intractable to derive the PDF for the sum of N cascaded Nakagami- m distribution $\chi_{1,k}$. Therefore, the random variable $\chi_{1,k}$ is approximated as a gamma distribution, denoted as $\Gamma(\mu, \eta)$ and its corresponding PDF and cumulative distribution function (CDF) are given by [16], [17], [18],

$$f_{\chi_{1,k}}(\chi_{1,k}) \approx \frac{\eta^\mu \chi_{1,k}^{\mu-1}}{\Gamma(\mu)} e^{-\eta \chi_{1,k}} \quad (4)$$

$$F_{\chi_{1,k}}(\chi_{1,k}) = \frac{\gamma(\mu, \eta \chi_{1,k})}{\Gamma(\mu)} = 1 - \frac{\Gamma(\mu, \eta \chi_{1,k})}{\Gamma(\mu)} \quad (5)$$

where $\mu = \frac{N\pi^2}{16-\pi^2}$ and $\eta = \frac{16-\pi^2}{4\pi}$, denote the shape and scale parameters, respectively. Furthermore, the CCI fading coefficients for all users $\chi_{2,k}$ are mutually independent and identically Gamma-distributed random variables. Therefore, the corresponding PDF and CDF are given by

$$f_{\chi_{2,k}}(\chi_{2,k}) = \frac{m^m}{\bar{\gamma}^m \Gamma(m)} \chi_{2,k}^{m-1} e^{-\frac{m \chi_{2,k}}{\bar{\gamma}}} \quad (6)$$

$$F_{\chi_{2,k}}(\chi_{2,k}) = \frac{\gamma\left(m, \frac{m}{\bar{\gamma}} \chi_{2,k}\right)}{\Gamma(m)} = 1 - \frac{\Gamma\left(m, \frac{m}{\bar{\gamma}} \chi_{2,k}\right)}{\Gamma(m)} \quad (7)$$

where m is the Nakagami fading parameter. $\Gamma(\cdot) = \Gamma(\cdot, 0)$ is the gamma function [19, eq. (8.3.10)], $\gamma(\cdot, \cdot)$ is the lower incomplete gamma function [19, eq. (8.350.1)], $\Gamma(\cdot, \cdot)$ is the upper incomplete gamma function [19, eq. (8.350.2)] and $\bar{\gamma} = \mathbb{E}[\chi_{2,k}]$, where $\mathbb{E}[\cdot]$ denotes the statistical expectation.

Using [20, eq. (3)], the ergodic capacity of the k th user can be expressed as

$$C_k = \mathbb{E} \left[\log_2 \left(1 + \frac{\rho \beta_k \chi_{1,k}}{\rho \tilde{\beta}_k \chi_{1,k} + \rho \chi_{2,k} + 1} \right) \right] \\ = \mathbb{E} \left[\frac{1}{\ln 2} \int_0^\infty \frac{1}{\tau} \left(1 - e^{-\tau \frac{\rho \beta_k \chi_{1,k}}{\rho \chi_{1,k} \tilde{\beta}_k + \rho \chi_{2,k} + 1}} \right) e^{-\tau} d\tau \right] \quad (8)$$

where $\tilde{\beta}_k = \sum_{i=k+1}^K \beta_i$ for $k \neq K$ and $\tilde{\beta}_k = 0$ for $k = K$. By using interchange of variables $z = \frac{\tau}{\rho\chi_{1,k}\tilde{\beta}_k + \rho_I\chi_{2,k} + 1}$ and some algebraic manipulations, (8) can be written as

$$C_k = \mathbb{E} \left[\int_0^\infty \frac{1}{z \ln 2} (1 - e^{-z\rho\beta_k\chi_{1,k}}) \times e^{-z(\rho\chi_{1,k}\tilde{\beta}_k + \rho_I\chi_{2,k} + 1)} dz \right]. \quad (9)$$

Using Fubini's theorem [21, p. 200], the expectation and integral can be swapped, hence (9) can be written as

$$C_k = \int_0^\infty \frac{e^{-z}}{z \ln 2} \left(1 - \underbrace{\mathbb{E} \left[e^{-z\rho\beta_k\chi_{1,k}} \right]}_{\mathcal{K}_1(z)} \right) \times \underbrace{\mathbb{E} \left[e^{-z(\rho\tilde{\beta}_k\chi_{1,k} + \rho_I\chi_{2,k})} \right]}_{\mathcal{K}_2(z)} dz \quad (10)$$

where $\mathcal{K}_1(z)$ and $\mathcal{K}_2(z)$ are the moment generating function (MGF) of $\chi_{1,k}$ and the joint MGF of $\chi_{1,k}$ and $\chi_{2,k}$ respectively. Using [19, eq. (6.451.2)] $\mathcal{K}_1(z)$, can be evaluated as

$$\begin{aligned} \mathcal{K}_1(z) &= \frac{\eta^\mu}{\Gamma(\mu)} \int_0^\infty \chi_{1,k}^{\mu-1} e^{\chi_{1,k}(-z\rho\beta_j + \eta)} d\chi_{1,k} \\ &= \left(1 + \frac{\rho\beta_k z}{\eta} \right)^{-\mu} \end{aligned} \quad (11)$$

where the integral in (11) is expanded using [19, eq. (6.451.2)]. Similarly, using the PDFs shown in (4) and (6), we obtain the joint MGF of $\chi_{1,k}$ and $\chi_{2,k}$ which is given as

$$\mathcal{K}_2(z) = \left(1 + \frac{\rho\tilde{\beta}_k z}{\eta} \right)^{-\mu} \left(1 + \frac{\rho_I\bar{\gamma}z}{m} \right)^{-m}. \quad (12)$$

By substituting (11) and (12) into (10), C_k evaluates to

$$\begin{aligned} C_k &= \frac{1}{\ln 2} \int_0^\infty \frac{e^{-z}}{z} \left(1 - \left(1 + \frac{\rho\beta_k z}{\eta} \right)^{-\mu} \right) \times \left(1 + \frac{\rho\tilde{\beta}_k z}{\eta} \right)^{-\mu} \left(1 + \frac{\rho_I\bar{\gamma}z}{m} \right)^{-m} dz. \end{aligned} \quad (13)$$

It is worth noting that (13) be evaluated numerically. Furthermore, by applying Laguerre orthogonal polynomial expansion, a closed-form expression for (13) can be expressed as

$$\begin{aligned} C_k &= \sum_{f=1}^F \frac{\mathcal{W}_f}{\mathcal{Z}_f \ln 2} \left[\left(1 - \left(1 + \frac{\rho\beta_k \mathcal{Z}_f}{\eta} \right)^{-\mu} \right) \times \left(1 + \frac{\rho\tilde{\beta}_k \mathcal{Z}_f}{\eta} \right)^{-\mu} \left(1 + \frac{\rho_I\bar{\gamma}\mathcal{Z}_f}{m} \right)^{-m} \right] + \mathcal{R}_F \end{aligned} \quad (14)$$

where \mathcal{W}_f , \mathcal{Z}_f and \mathcal{R}_F are the weight coefficients, sample points and remainder of the Lagurre polynomial which are tabulated in [22, Table 25.9].

Proposition 1: The Ergodic capacity of the k th user, for $1 < k \leq (K - 1)$ saturates to a ceiling at the high SNR

region. Thus, when $\rho \rightarrow \infty$, and using [7, eq. (31)], the ergodic capacity in (8) can be approximated as

$$\begin{aligned} C_k^\infty &= \log_2 \left(1 + \lim_{\rho \rightarrow \infty} \frac{\rho\beta_k\chi_{1,k}}{\rho\tilde{\beta}_k\chi_{1,k} + \rho_I\chi_{2,k} + 1} \right) \\ &= \log_2 \left(1 + \frac{\beta_k}{\tilde{\beta}_k} \right). \end{aligned} \quad (15)$$

From (15), it can be noted that the capacity ceiling or the maximum achievable rate is only affected by the power allocation coefficients, and it is independent of the fading channel conditions.

B. Outage Probability

This section presents the derived closed-form expressions for the outage probability performance. In the considered system, the outage event occurs when the k th user is unable to decode the j th user's signal correctly, that is defined as $O_{k,j} \triangleq \{R_{j \rightarrow k} < R\}$, $1 \leq j \leq k$, and $O_{k,j}^c$ is the complementary event of $O_{k,j}$. Therefore, the outage probability at the k th user can be written as

$$P_k^{out} = 1 - \Pr(O_{k,1}^c \cap \dots \cap O_{k,k}^c) \quad (16)$$

The outage event $O_{K,K}^c = \frac{\rho\chi_{1,K}\beta_K}{1+\chi_{2,K}} > \psi_K$, and the other outage event, $O_{k,j}^c$, for $1 \leq j \leq k$ can be expressed as

$$\begin{aligned} O_{k,j}^c &= \left\{ \frac{\rho\chi_{1,k}\beta_j}{1 + \chi_{2,k} + \rho\chi_{1,k} \sum_{i=j+1}^K \beta_i} > \psi_j \right\} \\ &= \left\{ \chi_{2,k} < \frac{\rho(\beta_j - \psi_j \sum_{i=j+1}^K \beta_i) - \psi_j}{\psi_j} \right\} \end{aligned} \quad (17)$$

where $\psi_j = 2^{R_j} - 1$, with R_j being the predefined target data rate. It should be noted that the k th user decodes the j th user signal when the following condition holds:

$$\beta_j > \psi_j \sum_{i=j+1}^K \beta_i. \quad (18)$$

Furthermore, denote $\phi_j \triangleq \frac{\psi_j}{\rho(\beta_j - \psi_j \sum_{i=j+1}^K \beta_i)}$ for $j < K$, $\phi_K \triangleq \frac{\psi_K}{\rho\beta_K}$, and $\phi_k^* = \max\{\psi_1, \dots, \psi_k\}$. Consequently, the outage probability can now be expressed as

$$P_k^{out} = \Pr(\chi_{2,k} < (\phi_k^* \chi_{1,k} - 1)). \quad (19)$$

Since $\chi_{1,k}$ is a random variable (RV), we cannot take the CDF directly. Therefore, we need to evaluate based on the conditional CDF of $\chi_{2,k}$. Hence, by using (5) and (6), the outage probability at the k th user can be expressed as follows

$$\begin{aligned} P_k^{out} &= \int_0^\infty F_{\chi_{2,k}}(\phi_k^* \chi_{1,k} - 1) \cdot f_{\chi_{1,k}}(\chi_{1,k}) d\chi_{1,k} \\ &= \frac{\eta^\mu}{\Gamma(m)\Gamma(\mu)} \int_0^\infty \underbrace{\gamma\left(m, \frac{m}{\bar{\gamma}}(\phi_k^* \chi_{1,k} - 1)\right)}_{\Xi} \times \chi_{1,k}^{\mu-1} e^{-\eta\chi_{1,k}} d\chi_{1,k}. \end{aligned} \quad (20)$$

By applying [19, eq. (8.3.52.6)], the lower incomplete gamma function in (20) and for integer values of m can be transformed into binomial expansion form as

$$\Xi = 1 - \Gamma(m) e^{-\frac{m}{\gamma}} (\phi_k^* \chi_{1,k} - 1) \sum_{b=0}^{m-1} \left(\frac{m}{\gamma} \right)^b \frac{(\phi_k^* \chi_{1,k} - 1)^b}{b!}. \quad (21)$$

The power of multinomial in (21) can be tackled by invoking [23, eq. (42)]

$$\sum_{b=0}^{m-1} \left(\frac{m}{\gamma} \right)^b \frac{(\phi_k^* \chi_{1,k} - 1)^b}{b!} = \Upsilon \left(\frac{m}{\gamma} \right)^P \sum_{i=0}^P \binom{P}{i} \chi_{1,k}^i \quad (22)$$

where

$$\Upsilon = \sum_{p_1=0}^{p_0} \sum_{p_2=0}^{p_1} \cdots \sum_{p_{m-1}=0}^{p_{m-2}} \frac{p_0!}{p_{m-1}!} \prod_{j=1}^{m-1} \left[\frac{(j!)^{p_{j+1}-p_j}}{(p_{j-1}-p_j)!} \right] \quad (23)$$

with $p_0 = 1$, $p_m = 0$, and $P = p_0 + p_1 + \cdots + p_{m-1}$.

By substituting (21) and (22) into (20), P_k^{out} is expressed as

$$P_k^{out} = \frac{\eta^\mu}{\Gamma(\mu)} \int_0^\infty \chi_{1,k}^{\mu-1} e^{-\eta \chi_{1,k}} d \chi_{1,k} - \eta^\mu \Upsilon \left(\frac{m}{\gamma} \right)^P \times \sum_{i=0}^P \binom{P}{i} \int_0^\infty \chi_{1,k}^{\mu+i-1} e^{-\frac{m \phi_k^* \chi_{1,k}}{\gamma}} d \chi_{1,k}. \quad (24)$$

The integrals in (24) can be evaluated using [19, eq. (3.326.2)], and P_k^{out} can now be expressed as

$$P_k^{out} = \frac{\eta^\mu}{\Gamma(\mu)} - \eta^\mu e^{-\frac{m}{\gamma}} \times \Upsilon \sum_{i=0}^P \binom{P}{i} \left(\frac{m \phi_k^* + \eta}{\gamma} \right)^{-(\mu+i)} \Gamma(\mu+i). \quad (25)$$

IV. NUMERICAL AND SIMULATION RESULTS

This section provides the performance of the considered IRS-aided NOMA system in terms of ergodic capacity and outage probability. Fixed power allocation technique is used in the simulations, and the parameters used to produce the results are $d_s = 2$ m, $d_{U_1} = 3$ m, $d_{U_2} = 2$ m, $d_{U_3} = 1$ m, $d_{L_l} = 10$ m, $\lambda = 3$, $m = 2$, $L = 3$ and $P_I = 10$ dBW. Monte Carlo simulations are incorporated to verify the accuracy of the derived analytical expressions and gain some insights into the system's performance. In each simulation run, 10^6 channel realizations are generated. In particular, all users are ordered by their distance from the IRS such that U_1 is the cell-edge user and U_2 and U_K are near users. We also investigate the impact of reflecting elements on the performance of IRS-aided NOMA and benchmark it with that of IRS-aided OMA system. Furthermore, the impact of CCI on user performance is demonstrated.

Fig. 2 shows the ergodic capacity versus SNR. It should be noted that the power allocation used are $\beta_1 = 0.7$, $\beta_2 = 0.25$ and $\beta_3 = 0.05$. The analytical results depicted in the figure are based on (13) and it is clear that they are in a good agreement with the simulated results. In addition, this further illustrates that the Gamma approximation closely matches the cascaded

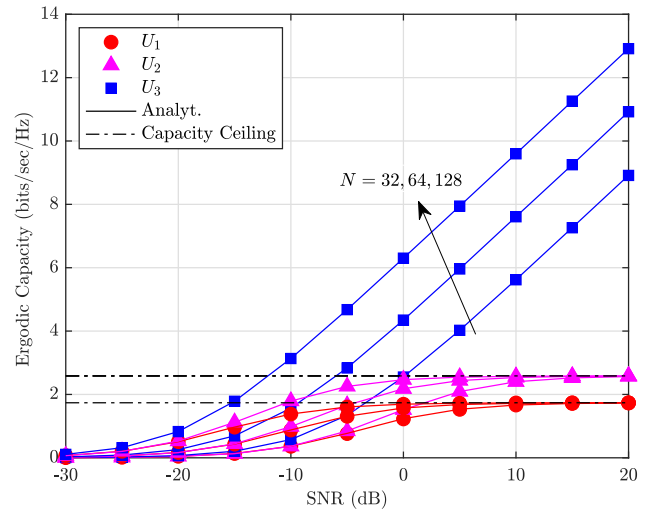


Fig. 2. Ergodic capacity.

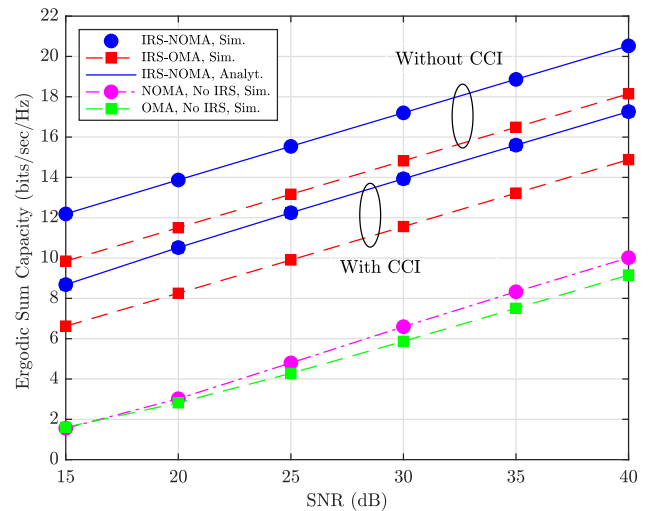


Fig. 3. Ergodic sum capacity.

Nakagami- m distribution. As can be seen from the figure, the ergodic capacity of U_1 and U_2 saturates to a capacity ceiling as the SNR value increases, which is confirmed in **Proposition 1**. The reason for this behavior is due to the fact that the user experiences inter-symbol interference from U_2 and U_3 when decoding its own signal. Another reason is the presence of the CCI in the network that substantially limits its achievable capacity. It is worth pointing out that the performance of U_1 , does not improve with varying N , particularly for $\rho \geq 20$ dB. However, it is only affected by the power allocation coefficient as demonstrated in **Proposition 1**. The difference in users' performance is due to the effect of inter-pair interference.

Fig. 3 depicts the ergodic sum capacity of the IRS-aided NOMA versus SNR. The proposed system results are benchmarked with conventional IRS-aided OMA and are produced by setting, $K = 2$, $N = 64$, $\beta_1 = 0.8$, $\beta_2 = 0.2$, $d_{U_1} = 3$ m and $d_{U_2} = 2$ m. The figure provides a comparison for both systems with and without CCI. It is clear that the performance of IRS-NOMA significantly outperforms IRS-OMA system for all SNR regions. For instance, when $\rho = 15$ dB the

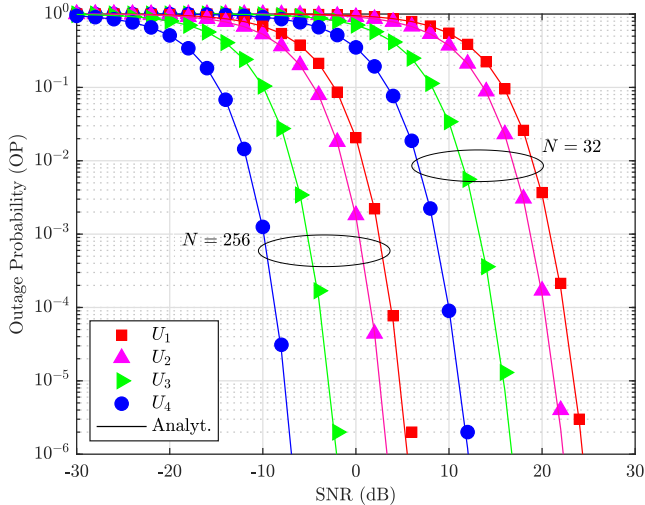


Fig. 4. Outage probability.

performance gain of IRS-aided NOMA for the interference-free case is 2.34 bps/Hz compared to its counterpart. This is due to the fact that NOMA enables efficient spectrum sharing by multiplexing users' signals within the same resource block. On the other hand, the presence of CCI limits the achievable rate to just 8.68 bps/Hz for IRS-NOMA and 6.62 bps/Hz for IRS-OMA. Furthermore, the achievable ergodic capacity of IRS-aided networks increases linearly as ρ approaches infinity. IRS can help facilitate ultra-reliable and efficient wireless communication links. Therefore, it is worth highlighting that IRS-NOMA can provide substantial performance gain even at extreme harsh conditions and interfering networks.

Finally, Fig. 4 shows the simulated and analytical outage probability versus SNR. The approximated outage probability curves are plotted according to (25) and they match well with the Monte simulation results. The results are produced by setting $\beta_1 = 0.75$, $\beta_2 = 0.18$ and $\beta_3 = 0.05$ and $\beta_4 = 0.02$. In this figure and for fair comparison, the predefined target data rate is set to 1 bps/Hz for all users. As can be seen from the figure, as N increases, lower outage probability are achieved for all K users. This is due to the fact that employing IRS to NOMA networks can provides a new means to improving the wireless link performance and enhancing the coverage.

V. CONCLUSION

This letter has studied an integrated IRS-NOMA system in Nakagami- m fading channels when taking into account cochannel interference. It derived the performance in terms of ergodic capacity and outage probability and demonstrated the validity of these expressions through comparisons with Monte Carlo simulations. It was shown that Gamma approximation closely represents the cascaded Nakagami- m distribution hence provides a powerful means to achieving closed-form expressions in complex scenarios. The results demonstrated the benefit of IRS in NOMA systems, and the relation between the number of reflecting elements and achievable rates.

REFERENCES

- [1] G. Yang, X. Xu, and Y.-C. Liang, "Intelligent reflecting surface assisted non-orthogonal multiple access," in *Proc. IEEE WCNC*, 2020, pp. 1–6.
- [2] Y. Liu et al., "Reconfigurable intelligent surfaces: Principles and opportunities," *IEEE Commun. Surveys Tuts.*, vol. 23, no. 3, pp. 1546–1577, 3rd Quart., 2021.
- [3] M. Al-Jarrah, A. Al-Dweik, E. Alsusa, Y. Iraqi, and M.-S. Alouini, "On the performance of IRS-assisted multi-layer UAV communications with imperfect phase compensation," *IEEE Trans. Commun.*, vol. 69, no. 12, pp. 8551–8568, Dec. 2021.
- [4] Q. Wu and R. Zhang, "Towards smart and reconfigurable environment: Intelligent reflecting surface aided wireless network," *IEEE Commun. Mag.*, vol. 58, no. 1, pp. 106–112, Jan. 2020.
- [5] Z. Ding et al., "On the performance of non-orthogonal multiple access in 5G systems with randomly deployed users," *IEEE Signal Process. Lett.*, vol. 21, no. 12, pp. 1501–1505, Dec. 2014.
- [6] A. Alqahtani, E. Alsusa, A. Al-Dweik, and M. Al-Jarrah, "Performance analysis for downlink NOMA over $\alpha-\mu$ generalized fading channels," *IEEE Trans. Veh. Technol.*, vol. 70, no. 7, pp. 6814–6825, Jul. 2021.
- [7] Y. Cheng, K. H. Li, Y. Liu, K. C. Teh, and H. V. Poor, "Downlink and uplink intelligent reflecting surface aided networks: NOMA and OMA," *IEEE Trans. Wireless Commun.*, vol. 20, no. 6, pp. 3988–4000, Jun. 2021.
- [8] L. Yuan, Q. Du, N. Yang, F. Fang, and N. Yang, "Performance analysis of IRS-aided short-packet NOMA systems over Nakagami- m fading channels," *IEEE Trans. Veh. Technol.*, vol. 72, no. 6, pp. 8228–8233, Jun. 2023.
- [9] S. Solanki, J. Park, and I. Lee, "On the performance of IRS-aided UAV networks with NOMA," *IEEE Trans. Veh. Technol.*, vol. 71, no. 8, pp. 9038–9043, Aug. 2022.
- [10] Z. Ding, R. Schober, and H. V. Poor, "On the impact of phase shifting designs on IRS-NOMA," *IEEE Wireless Commun. Lett.*, vol. 9, no. 10, pp. 1596–1600, Oct. 2020.
- [11] P. Yang, L. Yang, W. Kuang, and S. Wang, "Outage performance of cognitive radio networks with a coverage-limited RIS for interference elimination," *IEEE Wireless Commun. Lett.*, vol. 11, no. 8, pp. 1694–1698, Aug. 2022.
- [12] Z. Tang, T. Hou, Y. Liu, J. Zhang, and C. Zhong, "A novel design of RIS for enhancing the physical layer security for RIS-aided NOMA networks," *IEEE Wireless Commun. Lett.*, vol. 10, no. 11, pp. 2398–2401, Nov. 2021.
- [13] X. Yue, J. Xie, Y. Liu, Z. Han, R. Liu, and Z. Ding, "Simultaneously transmitting and reflecting reconfigurable intelligent surface assisted NOMA networks," *IEEE Trans. Wireless Commun.*, vol. 22, no. 1, pp. 189–204, Jan. 2023.
- [14] M. Mirahmadi, A. Al-Dweik, and A. Shami, "Interference modeling and performance evaluation of heterogeneous cellular networks," *IEEE Trans. Commun.*, vol. 62, no. 6, pp. 2132–2144, Jun. 2014.
- [15] A. Al-Dweik, A. Bedoui, and Y. Iraqi, "On the BER analysis of NOMA systems," Sep. 2023. [Online]. Available: https://www.techrxiv.org/articles/preprint/Comment_On_the_BER_Analysis_of_NOMA_Systems/24161586
- [16] Z. Yang, P. Xu, G. Chen, Y. Wu, and Z. Ding, "Performance analysis of IRS-assisted NOMA networks with randomly deployed users," *IEEE Syst. J.*, vol. 17, no. 2, pp. 1853–1864, Jun. 2023.
- [17] A.-A. Boulogeorgos and A. Alexiou, "Performance analysis of reconfigurable intelligent surface-assisted wireless systems and comparison with relaying," *IEEE Access*, vol. 8, pp. 94463–94483, 2020.
- [18] B. Tahir, S. Schwarz, and M. Rupp, "Analysis of uplink IRS-assisted NOMA under Nakagami- m fading via moments matching," *IEEE Wireless Commun. Lett.*, vol. 10, no. 3, pp. 624–628, Mar. 2021.
- [19] I. S. Gradshteyn and I. M. Ryzhik, *Table of Integrals, Series, and Products*, Cambridge, MA, USA: Academic Press, 2014.
- [20] K. A. Hamdi, "A useful lemma for capacity analysis of fading interference channels," *IEEE Trans. Commun.*, vol. 58, no. 2, pp. 411–416, Feb. 2010.
- [21] P. Billingsley, *Probability and Measure*. Hoboken, NJ, USA: Wiley, 2008.
- [22] M. Abramowitz and I. A. Stegun, *Handbook of Mathematical Functions With Formulas, Graphs, and Mathematical Tables*, vol. 55. Washington, DC, USA: U.S. Govt. Print. Office, 1968.
- [23] N. Yang, M. Elkashlan, and J. Yuan, "Outage probability of multiuser relay networks in Nakagami- m fading channels," *IEEE Trans. Veh. Technol.*, vol. 59, no. 5, pp. 2120–2132, Jun. 2010.